

# Seismic performance of self-centering bridge pier using seat angles

Rouzbeh Davoudi, Mehdi Ghassemieh and Mohammad Khanmohammadi

School of Civil Engineering, University of Tehran, Tehran, IRAN

e-mail: roozbeh\_davoudi@ut.ac.ir

## SUMMARY

*Recent earthquakes have demonstrated a need for a new design philosophy of retrofitting bridge piers aiming to avoid damage, ensure post-earthquake serviceability and reduce financial losses. Self-centering and rocking systems are mechanisms that help eliminate residual drift, maintain post-earthquake serviceability and reduce the possibility of bridge piers being demolished after earthquakes. The aim of this study is to evaluate the seismic performance of a self-centering bridge pier with seat angles as an energy absorption device in comparison with the traditional devices. In this regard, a series of nonlinear static and dynamic analyses on a typical, normal bridge pier and the proposed pier have been performed, and significant design criteria have been investigated. Energy absorption, ductility demand, residual and maximum drift have been investigated for both conventional and proposed pier. The results shed light on effect of rocking mechanism on the seismic enhancement of bridge piers.*

**Key words:** self-centering, bridge pier, seat angle, seismic performance, design philosophy, absorption device.

## 1. INTRODUCTION

The extensive damage to bridges during recent earthquakes, with tremendous human and economic losses from urban lifeline disruption, has led to a worldwide effort toward improving the seismic performance of bridges. In addition to the structural damage and the potential loss of life resulting from an earthquake, a severe economical impact is likely to result from the closure of bridges and disruption of the transportation infrastructure. Two key damage indicators, damage to plastic hinges and permanent drifts, need to be minimized in a new design or retrofit of bridges so that those may remain in service.

Traditional approaches to bridge design rely on the formation of flexural plastic hinges in bridge columns as a means of dissipation of seismic energy [1]. However, controlled rocking and self-centering systems in bridge piers can provide a method of seismic resistance, resulting in significantly less damage

following strong motions. The use of controlled rocking and self-centering systems at column ends provides a means of reducing the sustained damage and residual offset in bridge systems.

This paper evaluates a self-centering bridge pier with seat angles as energy absorption device along with unbonded, post-tensioned cable in comparison with a traditional pier.

### 1.1 Self-centering and controlled rocking systems in bridge piers

The role of a self-centering system is to minimize the residual displacements of a bridge system following a seismic event. This role is accomplished by including an element that remains elastic throughout the event and that provides the system with a restoring force. High-strength, unbonded, post-tensioned cables have typically been used for this purpose. Being

unbonded, the cables are free to move relative to the concrete, so that the extension of the bar length is distributed over the whole unbonded length. This allows the system to reach a larger displacement without yielding the restoring element. In fact, using post-tensioned unbonded tendons rather than bonded ones, means that strains in the post-tension rods are not localized and smaller tendons can be used.

Mander and Cheng [2] have proposed rocking, concrete bridge columns as a seismic resistant system consistent with a design methodology called Damage Avoidance Design (DAD). According to this concept, each bridge column is allowed to rock individually by making the rebar discontinuous at the column ends, thus allowing rocking at the column/cap beam and column/foundation beam interfaces. The columns are subsequently designed as pre-cast elements, post-tensioned vertically to increase and control the lateral strength. Palermo et al. [3] have proposed the use of a hybrid system for concrete bridge piers that uses vertical post-tensioning of the concrete bridge columns and different forms of energy dissipation devices (hysteretic, friction, and visco-elastic). In their study, a displacement based approach has been presented for the design of both bridge piers and/or bridge systems. Marriott et al. [4] have investigated experimentally and analytically these hybrid connections for the seismic resistance of concrete bridges. Quasi-static and pseudo-dynamic testing have confirmed the desired performance of the connection that included no “physical” damage and the self-centering ability. Mahin et al. [5] have proposed a new post-tensioning design to minimize residual displacements in columns, in which a longitudinal post-tensioning tendon has been utilized and replaced with some of the usual longitudinal mild reinforcing bars.

## 1.2 Energy dissipation systems in bridge piers

To overcome the drawback of a low hysteretic energy dissipation capacity, additional energy dissipaters have been used to increase the hysteretic damping of the system. In most cases, hysteretic damping comes from the yielding of the steel element. Energy dissipaters can be divided into two main categories: internal and external (fuses) energy dissipation systems. Chang et al. [6] and Ou et al. [7] have used mild steel bars between pier segments as internal energy dissipaters. The bars have proved their efficiency by significantly increasing the hysteretic energy dissipation. The major problem with this type of energy dissipater is that, after yielding, the bars remain permanently deformed and, after loading, the whole system suffers from a permanent residual displacement.

Chou and Chen [8] have provided one of their piers

with a dog bone shaped external energy dissipater. They have reported that their system has increased the equivalent viscous damping of the system from 6.5% to 9%. Marriott et al. [9] have used two different layouts of external energy dissipater systems for segmental piers. They have used mild steel bars encased in steel confining tubes that have been injected with epoxy to obtain a fuse-like behaviour and to be able to dissipate energy while subjected to tension and/or compression stresses. ElGawady et al. [10] have used external steel angles and rubber pads as external energy dissipaters and isolation dissipation devices respectively.

Overall, the external energy absorption devices have proved to have the advantage of being easily changed and, hence, have not increased the residual drift of the system.

## 2. HYSTERETIC BEHAVIOUR OF SEAT ANGLES

Shen and Astanteh-Asl [11] have conducted monotonic and cyclic loading tests on isolated angles. On the basis of the conducted tests, it has been concluded that the bolted-angle connections demonstrate stable cyclic response and reliable energy dissipation capacity. The increase in strength has been attributed to the combined effect of large deformations and material strain hardening. The cyclic ductility of the specimens has been reported to range from 8 to 10. In other experimental works [12-15] studies have been performed to evaluate the post tension connection with seat angles. The effects of altering different parameters such as the thickness and gauge length of the angles and the post-tensioning steel have been explored.

### 2.1 Hysteretic behaviour of seat angle model

Shen et al. [16] have modelled the top and seat angles in beam to wall connection. In their model, they have assumed that the failure of the angle occurs through the formation of two plastic hinges in the vertical leg; as shown in Figure 1.

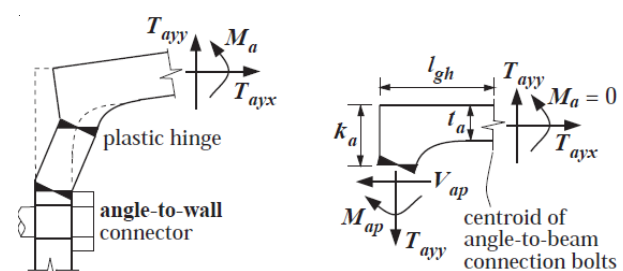


Fig. 1 Deformed shape and body diagram of the angle

In Figure 1, from the free body diagram of the angle between the plastic hinge adjacent to the fillet on the vertical leg and the centroid of the angle-to-beam connection bolts, it is observable that:

$$T_{ayx} = V_{ap} \quad (1)$$

$$M_{ap} = \frac{V_{ap} l_{g2}}{2} \quad (2)$$

$$V_{ap} = \frac{f_{ay} l_a t_a}{2} \quad (3)$$

in which,  $T_{ayx}$  is axial force in the angle horizontal,  $M_{ap}$  is plastic hinge moment,  $V_{ap}$  is plastic shear force in the vertical leg including shear-flexure interaction,  $f_{ay}$  is yield strength of the angle steel,  $l_a$  is length of angle,  $t_a$  is angle leg thickness and  $l_{g2}$  is effective gage length for assumed plastic hinge mechanism. Under tensile loading, the yield strength is equal to  $V_{ap}$ . Initial stiffness ( $K_{aixt}$ ) has been determined using a method developed by Kishi and Chen [17] and Lorenz et al. [18]:

$$\frac{l_{g2}}{t_a} \left( \frac{V_{ap}}{V_{a0}} \right) + \left( \frac{V_{ap}}{V_{a0}} \right)^4 = 1 \quad (4)$$

$$K_{aixt} = \frac{3E_a I_a}{l_{g1} (l_{g1}^2 + 0.78t_a^2)} \quad (5)$$

In this model, the vertical leg has been assumed to be fixed along the innermost edge of the line of angle-to-beam connectors and is pulled horizontally by the beam.

In the above equations,  $E_a I_a$  is a flexural stiffness of angle,  $t_a$  is the thickness of angle and  $l_{g1}$  is the length of the vertical leg that has been assumed to act as cantilever.

Based on the Shen et al. [16] study, it has been assumed that the maximum strength of the horizontal angle element in tension ( $T_{asx}$ ) equals to 2 times the yield strength ( $T_{ayx}$ ) and is reached at an angle deformation ( $\delta_{asx}$ ) of 5 times the yield deformation. Under compression, the initial stiffness of an angle, as it is pushed back horizontally toward the wall by the coupling beam, has been assumed to be equal to:

$$K_{aixc} = \frac{1}{40} \cdot \frac{E_a A_a}{l_{gh}} \quad (6)$$

in which,  $E_a$  is Young's modulus for the angle steel,  $A_a$  is gross cross-section area of the angle horizontal  $l_{eg}$  and  $l_{gh}$  are gage length of the angle-to-beam connectors (measured from the heel of the angle to the centroid of the angle-to-beam connection bolts). In Shen et al. [16], the unloading stiffness has been assumed to be equal to the initial stiffness ( $\gamma_{unl}=1$ ) for the modelling of steel, unbonded, post-tensioned coupling beams. Upon crossing the zero-force axis, the angle force-deformation behaviour shoots towards the angle yield strength in compression ( $C_{ayx}$ ) which

has been assumed to be equal to 0.75 times the initial slip critical force, ( $C_{asi}$ ) of the angle-to-beam connection bolts. The 0.75 factor accounts for the losses that occur in the clamping forces of the angle-to-beam connection bolts and the resulting losses in the slip critical force as the structure undergoes large lateral displacements. In the compression angle, the beam corner comes into contact with the wall. Note that the slip of the angle-to-beam connection bolts can also occur when the angle is pulled away from the wall, though this is not a desirable type of behaviour. It has been assumed that the slip critical capacity of the angle-to-beam connection bolts ( $C_{as}=0.75C_{asi}$ ) is larger than the angle capacity in tension ( $1.25T_{ayx}$ ); and thus, slip does not occur in tension. The angle-to-beam connections should be designed to ensure this behaviour.

Hysteretic behaviour of seat angle that has been proposed by Shen et al. [16] is presented in Figure 2.

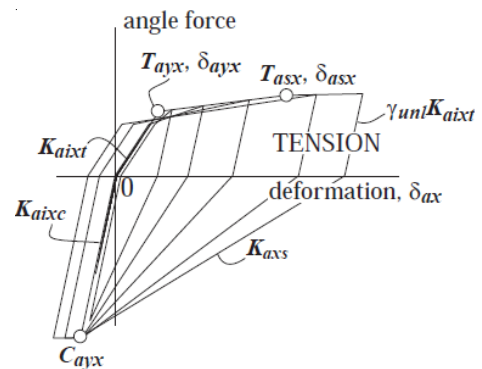


Fig. 2 Hysteretic behaviour of seat angles model by Shen et al. [16]

In this study, the model of Shen et al. [16] is utilized to model the behaviour of seat angles as an external energy absorption device.

### 3. REFERENCE BRIDGE PIER

A one-quarter scaled, conventional, reinforced concrete bridge pier with flexural-shear behaviour and experimental, static cyclic results has been selected as the reference bridge [19]. The conventional bridge pier is modelled analytically to be comparable with the proposed bridge pier.

The geometric as well as mechanical specifications of the bridge pier are as follows: the diameter and length of the pier are 307 mm and 895 mm respectively, cover to center of the hoop bar is 36 mm, the axial force on the pier is 10% of the section capacity, the longitudinal reinforcement ratio is 1.83%, the diameter of the spirals is 6 mm with a spacing of 75 mm, the compression strength of unconfined concrete is 34.4 MPa and the yield strength of longitudinal and transverse steel are 240 MPa.

### 3.1 Modelling of the reference bridge pier

The 2-D finite element model of the reference bridge pier, as well as the test setup, has been developed and analyzed using an open-source, finite element program OpenSees [20]. The plastic hinge approach with Clough material, which has been developed and implemented in the OpenSees material library, has been utilized for analytical modelling. Plastic hinge length has been obtained according to the Eq. (7) [21], in which  $L$ ,  $d_b$  and  $f_y$  are column length, diameter and tensile strength of longitudinal bars respectively. The moment and rotations have been obtained according to the bending capacity of column and flexural-shear interaction respectively. Moreover, the parameters of Clough material have been obtained according to the recommendations of Haselton et al. [22]. In this regard, next equations predicts a normalized energy-dissipation capacity,  $\lambda$ , in which  $s/d$  and  $v$  are the ratio of stirrup spacing to column depth and axial load ratio respectively:

$$L_p = 0.08L + 0.022f_y d_b \quad (7)$$

$$\lambda = (170.7) (0.27)^v (0.1)^{s/d} \quad (8)$$

In addition, a degrading parameter,  $c$ , has been considered 1.2, given the flexural behaviour of the reference bridge pier. The analytical and experimental results are shown in Figure 3. The analytical results has been verified with an experimental test.

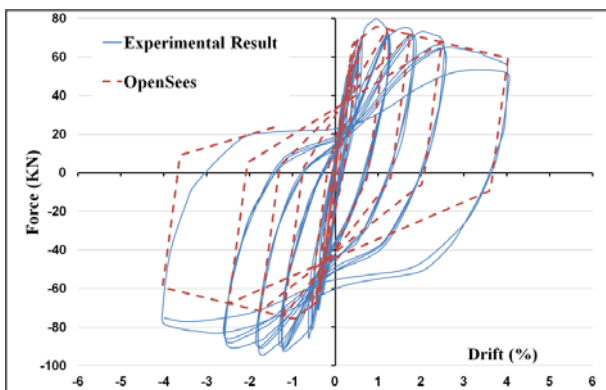


Fig. 3 Calibration of the reference bridge pier

## 4. PROPOSED BRIDGE PIER

The proposed bridge pier has been allowed to rock by making the rebar discontinuous at the column ends. The pier has been post-tensioned vertically with an unbonded cable in order to control the lateral strength and decrease residual drift. For a more accurate comparison, geometrical dimensions and other mechanical properties of the proposed model material have been considered to be the same as that of the conventional pier. Four external seat angles have been

connected to steel jacket to enhance energy absorption in the controlled rocking zone. Steel jacket has been used at the end of the pier for making a better connection between the seat angles and the pier and for the improvement of the rocking behaviour by confining rocking zone. In order to reach minimum residual drift and less damage, instead of seat angles, pier must remain elastic. Thus, the dimensions of seat angles have to be limited to the point where the yielding of the fuses takes place earlier than pier. The post-tensioning force has been set to be less than 40% of the yield force of the post-tensioned cable. The yield strength of the cable and seat angles have been assumed to be 1792 MPa and 352 MPa respectively and the area of post-tension cable has been assumed to be 1 cm<sup>2</sup>. In this study, the dimensions of seat angles have been chosen to be of L200\*120\*19 and L200\*120\*14 with a length of 150 mm. Post-tensioned ratio, defined as a ratio between cable force and section capacity, has been chosen to be 0, 1, and 3 %. The scheme of the proposed pier is illustrated in Figure 4.

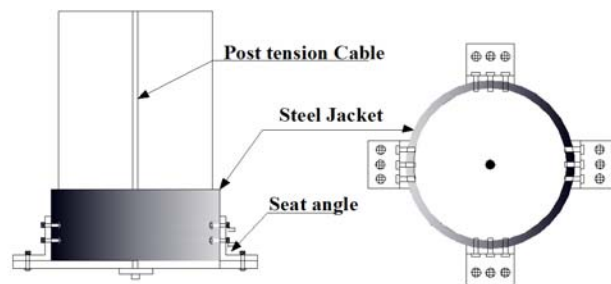


Fig. 4 Scheme of the proposed rocking pier

### 4.1 Numerical modelling of the proposed bridge pier

Modelling of the proposed bridge pier has been carried out using OpenSees [20]. The segment of the pier without a steel jacket has been modelled using nonlinear, beam column element separated into steel, confined and unconfined concrete fibers. The segment of the pier with a steel jacket has also been modelled using nonlinear, beam column element separated into steel and confined concrete fibers. In order to consider the effect of the steel jacket confining in the entire section, the rocking zone has been modelled using a zero length element section with concrete material. Hysteretic behaviour of the seat angle, as shown in Figure 2, has been modelled with hysteretic material in OpenSees. Horizontal shear has been assumed to be transferred from the connections of the column to the foundations because seat angles are sufficient for this purpose. The post-tensioned cable has been modelled with truss element using initial strain material existing in OpenSees library.

### 5. STATIC CYCLIC ANALYSIS

The results indicate that, when subjected to a static, cyclic loading, energy absorption in the proposed bridge pier is lower than in the conventional bridge pier. However, other structural elements remain elastic in the new bridge pier. Increasing the thickness of seat angles results in more energy absorption, which leads to the nonlinear behaviour of the pier. On the other hand, using  $L200*120*19$  seat angles as energy absorption devices causes the ductility capacity to increase to 9. In Figure 5, the cyclic behaviour of the rocking pier with  $L200*120*19$  seat angles and without a cable, and the conventional bridge pier is shown, in which the self-centering behaviour of the rocking pier is easily observable.

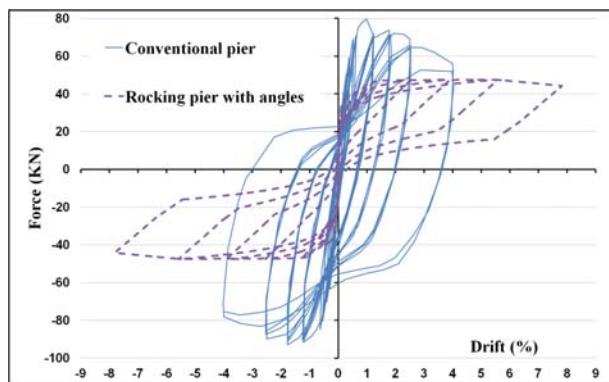


Fig. 5 Cyclic behaviour of rocking pier with  $L200*120*19$  seat angles and conventional pier

A comparison of the cyclic behaviour of the rocking piers with  $L200*120*19$  seat angles under an axial load ratio of 5%, with a post-tensioning force ratio of 3% and with and without post-tensioned cable is illustrated in Figure 6. As shown in Figure 5, the lateral strength of a rocking pier is increased by the presence of a post-tensioned cable.

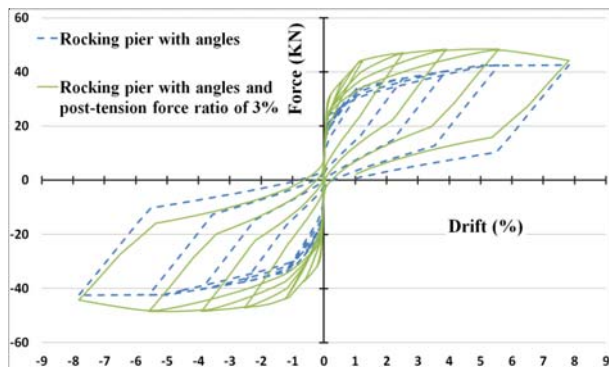


Fig. 6 Cyclic behaviour of rocking pier with  $L200*120*19$  seat angles and rocking pier with angles and post-tensioned cable

### 6. TIME HISTORY ANALYSIS

In order to assess the realistic behaviour of the proposed bridge pier, the bridge pier with  $L200*120*19$

seat angle with 3% post-tensioning load ratio has been compared with the conventional bridge pier. In addition, a nonlinear dynamic analysis has been conducted using seven far-field ground motion records. The ground motions which have been used in this study have been selected from Pacific Earthquake Engineering Center (PEER) strong motion data base. Seven far ground motions have been chosen and scaled to the MCE seismic level. These records have been selected according to their characteristics such as fault rupture mechanism and site classification so as to be similar to the previously mentioned structure. The records have been assembled and scaled to match the design response spectrum for the San Francisco Bay Area region. The ground motions correspond to site class *D* in AASHTO-2010 [23]. Using 7% probability of exceedance in 75 years seismic hazard maps with soil profile type *D* and acceleration coefficient equalling  $0.55 g$ , the MCE design response spectrum has been developed according to AASHTO-2010 [23].

For scaling, the geometric-mean scaling method has been used. This method involves amplitude scaling of a pair of seed motions by a single factor to minimize the sum of the squared errors between the target spectral values and the geometric mean (square root of the product, hereafter termed *geomean*) of the spectral ordinates for the pair at appropriate periods. This scaling procedure seeks to preserve the record-to-record dispersion of spectral ordinates and the spectral shapes of the seed ground motions. In this study, since 2-D dynamic analysis has been carried out, one component of motion should be considered in order to minimize the sum of the squared errors between the target spectral values and ground motion spectrum.

Each of the seven motions has been scaled in amplitude only by factor  $F_j$  in the period range of  $0.5T$  to  $2.0T$ , in which  $T$  is a fundamental period of the bridge. Put simply, geometric mean approach has been utilized so as to minimize the error,  $E_j$ , between the scaled motion spectrum,  $F_j S_{FN}$ , and the target spectrum,  $S_{DE}$ :

$$S_j = \sum [S_{DE}(T_i) - F_j S_{FN}(T_i)]^2 \tag{9}$$

The equation results in the following direct expression for the scale factor,  $F_j$ :

$$F_j = \frac{\sum [S_{DE}(T_i) - S_{FN}(T_i)]}{\sum [S_{FN}(T_i)^2]} \tag{10}$$

To meet the acceptable criteria of AASHT 2010 [23], the envelope of a median spectra from all horizontal far and near-field records have been separately controlled so that they do not fall below corresponding ordinate of the response spectrum in the period range of  $0.5T$  to  $2.0T$ . The characteristics of seven far field ground motions and scale factors are described in Table 1.

Table 1. Ground motions

No	Earthquake	Station	Soil type	PGA (g)	PGV (cm/s)	Scale factor
1	Imperial Valley	5053 Calexico Fire Station	D	0.275	21.2	2.08
2	Imperial Valley	117 El Centro Array #9	D	0.313	29.8	1.82
3	Landers	22074 Yermo Fire Station	D	0.245	51.5	3.07
4	Morgan Hill	57382 Gilroy Array #4	D	0.348	17.4	1.90
5	Superstitt Hills(B)	11369 Westmorland Fire Station	D	0.211	31.0	2.78
6	Superstitt Hills(B)	01335 El Centro Imp. Co. Cent	D	0.358	46.4	1.82
7	Westmorland	5169 Westmorland Fire Station	D	0.496	34.4	1.54

Figure 7 shows a comparison between the code-based design response spectrum and the average response spectrum of the seven far-field ground motion records after they have been scaled.

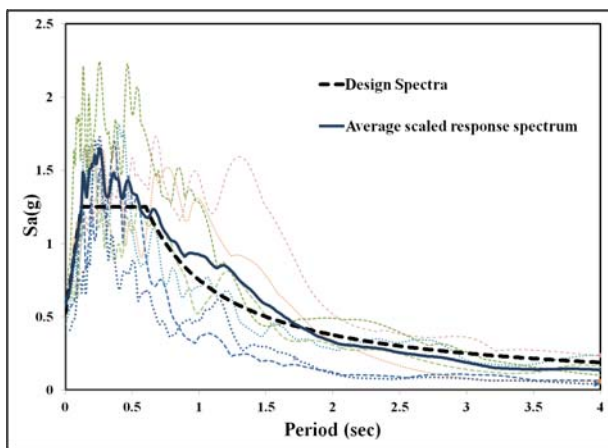


Fig. 7 Design response spectrum used in the analysis compared to the scaled spectra of the ground motions' set

It should be noted that, for all records, analysis was performed according to one-quarter geometric scaling factor of the conventional and proposed pier. Afterwards, time intervals of the records have been scaled to 0.5. Time history results demonstrate beneficial characteristics of the rocking pier in comparison with the conventional one. The rocking pier minimizes residual drift as well as the total energy demand of ground motions. However, the displacement demand can be increased in comparison with the conventional pier. To provide a better understanding of the effectiveness of rocking mechanism in the innovative pier, the hysteretic behaviour and drift history response of the Landers earthquake for the rocking pier with  $L200*120*19$  seat angle with 3% post-tensioning load ratio and the conventional pier are presented in Figures 8 and 9. Figure 8 indicates a stable energy absorption in the rocking pier in comparison with the traditional one. Moreover, the total energy absorption demand in the rocking pier is much less than in the conventional one. In other words, the rocking mechanism enhances effective damping, and decreases input energy of ground motions. In addition,

as shown in Figure 9, the rocking mechanism, along with a post-tensioned cable, brings about minor residual drift, and the proposed pier is able to withstand a strong ground motion without considerable residual drift. On the other hand, during a ground motion, the rocking pier experiences lower base shear force in comparison with the flexural column. Undoubtedly, these beneficial features of the proposed pier guarantee a good seismic performance of bridge systems.

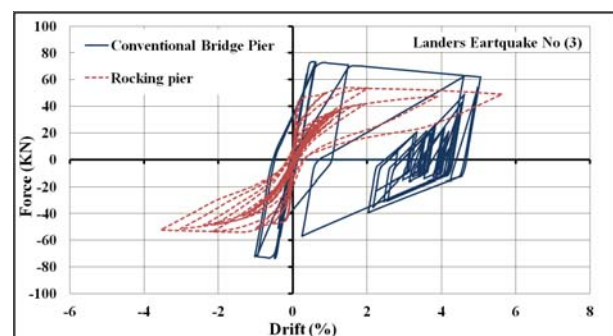


Fig. 8 Hysteretic behaviour results of conventional and rocking pier in Landers records

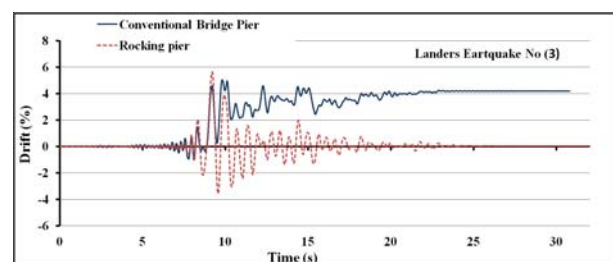


Fig. 9 Drift history results of conventional and rocking pier in Landers records

For all seven far-field records, the time history analysis has been carried out for both systems in order to evaluate the seismic performance of the proposed and conventional pier. In this regard, energy absorption, ductility demand, maximum drift and residual drift have been studied in all records.

The total hysteretic energy absorption for both systems is described in Figure 10. Results show the proposed pier experiences much less input energy in comparison with the conventional one, in the all

records. The average of the total hysteretic energy in the rocking pier is about one-third of the total hysteretic energy average in the conventional pier. As Figure 11 shows, the residual drifts in the rocking pier are much less than in the conventional pier. The average residual drift for all records in the rocking and traditional pier are 0.2% and 2% respectively. Given that the energy absorption in the rocking pier is much lower than in the conventional one, the rocking pier tends to experience larger displacements in comparison with the traditional pier. Figure 12 illustrates the maximum drift for both systems in all records. The average maximum experienced drifts for both rocking and conventional pier are 5% and 4% respectively. In order to assess ductility demand in the proposed pier in comparison with the flexural pier, ductility demand in the proposed pier has been defined as a ratio of maximum drift to the drift corresponding to yield of seat angles. Figure 13 shows the ductility demand for both systems in all seven records. The average ductility demands for the innovative and conventional piers are 5% and 4.7% respectively.

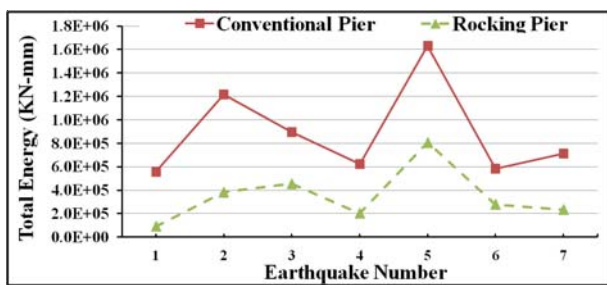


Fig. 10 Total energy demand

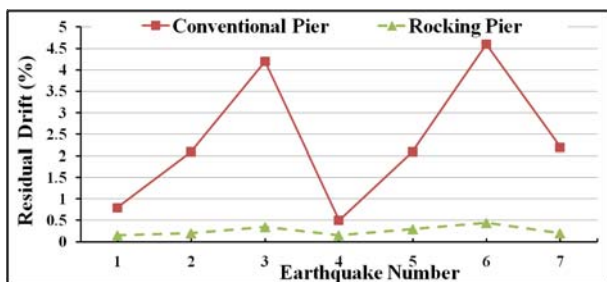


Fig. 11 Residual drift

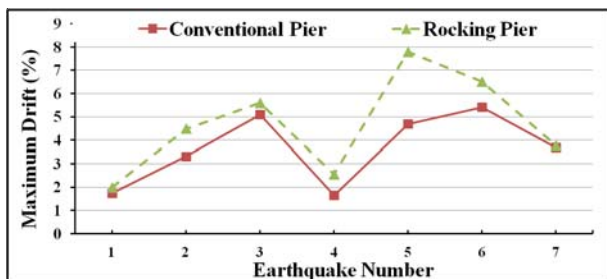


Fig. 12 Maximum drift

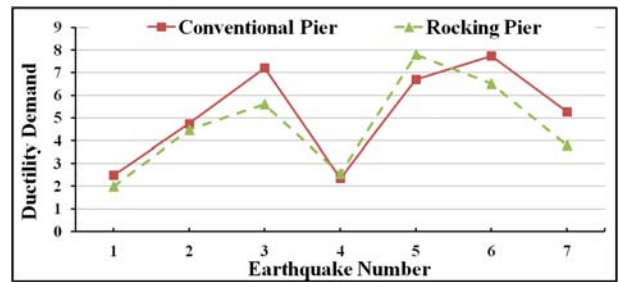


Fig. 13 Ductility demand

## 7. CONCLUSION

Large lateral drift capacity (8%) of the proposed bridge pier is the major advantage in comparison with the conventional one (5%). The cyclic behaviour of the rocking pier demonstrates a stable cyclic response and reliable energy dissipation capacity in which strength degradation does not occur. Rocking mechanism ushers in less shear force demand in comparison with the fixed pier. In this study, the employment of the rocking mechanism in the proposed rocking pier results in a decrease of 70% of the flexural pier base shear. Consequently, this advantage could lead to reduction in production costs by constructing lighter foundations. The lack of structural damage in other parts of the pier due to large displacements is yet another benefit of the rocking pier. The external seat angles have the advantage of being easily changed and, hence, cost of repair and retrofitting is minimized after an earthquake. To reach this aim, the dimension of seat angles should be designed according to the capacity of the pier; hence, other parts could be elastic and no damage would occur in its other parts.

The post-tensioned cable accounts for a self-centering behaviour: time history results indicate that the proposed bridge pier experiences an average residual drift of 0.3%. Hence, the proposed pier ensures post-earthquake serviceability. However, the conventional pier is prone to experience major residual drifts of 2-5%. Moreover, the results have shed light on the possibility of the rocking mechanism to decrease seismic energy demand. The results indicate that the rocking mechanism can diminish the earthquake demand to one-third of the seismic energy demand. Due to a lower amount of energy absorption capacity in the rocking pier in comparison with the conventional one, the rocking pier is likely to experience more drift in order to absorb input energy. The results of seven far-field records illustrate that the average maximum experienced drifts of the self-centering pier is 1% higher than the average maximum experienced drifts of the conventional one (4%). However, the total energy absorption in the rocking pier is about one-third of the conventional pier energy absorption.

## 8. REFERENCES

- [1] AASHTO, LRFD Bridge Design Specifications, 3<sup>rd</sup> edition, American Association of State Highway and Transportation Officials, Washington, 2005.
- [2] J.B. Mander and C.-T. Cheng, Seismic Resistance of Bridge Piers Based on Damage Avoidance Design, Technical Report NCEER-97-0014, National Center for Earthquake Engineering Research, The State University of New York at Buffalo, Buffalo, 1997.
- [3] A. Palermo, S. Pampanin and G.M. Calvi, Concept and development of hybrid solutions for seismic resistant bridge systems, *Journal of Earthquake Engineering*, Vol. 9, No. 6, pp. 899-921, 2005.
- [4] D. Marriott, A. Palermo and S. Pampanin, Quasi-static and pseudo-dynamic testing of damage resistant bridge piers with hybrid connections, Proc. of the 1<sup>st</sup> European Conf. on Earthquake Engineering and Seismology - ECEES, Geneva, Curran Associates, Inc., pp. 4314-4323, 2006.
- [5] S.A. Mahin, J. Sakai and H. Jeong, Use of partially prestressed reinforced concrete columns to reduce post-earthquake residual displacements of bridges, Proc. of the 5<sup>th</sup> National Seismic Conference on Bridges & Highways, San Francisco, Paper No. B25, 2006.
- [6] K.C. Chang, C.H. Loh, H.S. Chiu, J.S. Hwang, C.B. Cheng and J.C. Wang, Seismic Behavior of Precast Segmental Bridge Columns and Design Methodology for Applications in Taiwan, Taiwan Area National Expressway Engineering Bureau, Taipei, 2002. (in Chinese)
- [7] Y.-Ch. Ou, M. Chiewanichakorn, A.J. Aref and G.C. Lee, Seismic performance of segmental precast unbonded posttensioned concrete bridge columns, *ASCE Journal of Structural Engineering*, Vol. 133, No. 11, pp. 1636-1647, 2007.
- [8] Ch.-Ch. Chou and Y.-Ch. Chen, Cyclic tests of post-tensioned precast CFT segmental bridge columns with unbonded strands, *Earthquake Engineering and Structural Dynamics*, Vol. 35, No. 2, pp. 159-175, 2006.
- [9] D. Marriott, S. Pampanin and A. Palermo, Quasi-static and pseudo-dynamic testing of unbonded post-tensioned rocking bridge piers with external replaceable dissipaters, *Earthquake Engineering and Structural Dynamics*, Vol. 38, No. 3, pp. 331-354, 2009.
- [10] M. ElGawady, A.J. Booker and H.M. Dawood, Seismic behavior of posttensioned concrete-filled fiber tubes, *ASCE Journal of Composites for Construction*, ASCE, Vol. 14, No. 5, pp. 616-628, 2010.
- [11] J. Shen and A. Astaneh-Asl, Hysteretic behavior of bolted-angle connections, *Journal of Constructional Steel Research*, Vol. 51, No. 3, pp. 201-218, 1999.
- [12] J.M. Ricles, R. Sause, S.W. Peng, and L.W. Lu, Experimental evaluation of earthquake resistant posttensioned steel connections, *ASCE Journal of Structural Engineering*, Vol. 128, No. 7, pp. 850-859, 2002.
- [13] P. Rojas, J.M. Ricles and R. Sause, Seismic performance of post-tensioned steel moment resisting frames with friction devices, *ASCE Journal of Structural Engineering*, Vol. 131, No. 4, pp. 529-540, 2005.
- [14] M.E.M. Garlock, Full-scale testing, seismic analysis, and design of post-tensioned seismic resistant connections for steel frames. Ph.D. Thesis, Department of Civil and Environmental Engineering, Lehigh University, Bethlehem, 2002.
- [15] M.M. Garlock, J.M. Ricles and R. Sause, Experimental studies of full-scale posttensioned steel connections, *ASCE Journal of Structural Engineering*, Vol. 131, No. 3, pp. 438-448, 2005.
- [16] Q. Shen, Y.C. Kurama and B.D. Weldon, Seismic design and analytical modeling of posttensioned hybrid coupled wall subassemblages, *ASCE Journal of Structural Engineering*, Vol. 132, No. 7, pp. 1030-1040, 2006.
- [17] N. Kishi and W.-F. Chen, Moment-rotation relations of semirigid connections with angles, *ASCE Journal of Structural Engineering*, Vol. 116, No. 7, pp. 1813-1834, 1990.
- [18] R.F. Lorenz, B. Kato and W.-F. Chen (Eds.), *Semi-Rigid Connections in Steel Frames*, Council on Tall Buildings and Urban Habitat, Committee 43, McGraw-Hill, Inc., New York, 1993.
- [19] J. Petrovski and D. Ristić, Reversed Cyclic Loading Test of Bridge Column Models, Report IZIIZ 84-164, Institute of Earthquake Engineering and Engineering Seismology, Skopje, 1984.
- [20] S. Mazzoni, F. McKenna, M.H. Scott and G.L. Fenves, *OpenSees Command Language Manual*, College of Engineering, University of California, Berkeley, 2007.
- [21] M.J.N. Priestley, F. Seible and G.M. Calvi, *Seismic Design and Retrofit of Bridges*, John Wiley & Sons Inc., New York, 1996.
- [22] C.B. Haselton and G.G. Deierlein, Assessing Seismic Collapse Safety of Modern Reinforced Concrete Frame Buildings, PEER Report 2007/08, Pacific Engineering Research Center, University of California, Berkeley, 2007.
- [23] AASHTO, LRFD Bridge Design Specifications, 5<sup>th</sup> edition, American Association of State Highway and Transportation Officials, Washington, 2010.

## POBOLJŠANJE POTRESNOG PONAŠANJA SAMOCENTRIRAJUĆEG STUPA MOSTA UPORABOM KUTNIH PROFILA

### SAŽETAK

*Potresi kojima smo svjedočili u posljednje vrijeme ukazali su na potrebu za novim pristupom pri projektiranju obnove stupova mostova čijom bi se primjenom izbjegla oštećenja, osigurala adekvatna uporabljivost mosta nakon djelovanja potresa te umanjio financijski trošak. Korištenjem sustava temeljenih na samocentriranju (self-centering) i kontroliranom ljuľljanju (controled rocking) bi se eliminirali zaostali pomaci, sačuvala mogućnost uporabljivosti mosta te umanjila mogućnost njegova urušavanja nakon djelovanja potresa. Cilj ovoga rada je procjena potresnog odgovora samocentrirajućih stupova mostova s kutnim profilima kao sredstvima apsorpcije energije u usporedbi s klasičnim mehanizmima apsorpcije odnosno apsorpcijskim uređajima. U tu svrhu, proveden je niz nelinearnih statičkih i dinamičkih analiza kako na klasičnom tako i na novopredloženom tipu stupa mosta te su istraženi relevantni kriteriji pri projektiranju. Apsorpcija energije, zahtjevana duktilnost, zaostali i maksimalni pomaci su istraženi za konvencionalni i novopredloženi tip stupa. Rezultati pružaju bolji uvid u posljedice koje upotreba mehanizma utemeljenog na mehanizmu kontroliranog ljuľljanja može imati na poboljšanje seizmičkog ponašanja stupova mostova.*

**Ključne riječi:** *samocentriranje, stup mosta, kutni profil, potresno ponašanje, filozofija projektiranja, apsorpcijski uređaj.*